AIChE

Detailed Kinetic Analysis of Oil Shale Pyrolysis TGA Data

Pankaj Tiwari and Milind Deo
Dept. of Chemical Engineering, University of Utah, Salt Lake City, UT 84102

DOI 10.1002/aic.12589
Published online March 22, 2011 in Wiley Online Library (wileyonlinelibrary.com).

There are significant resources of oil shale in the western United States, which if exploited in an environmentally responsible manner would provide secure access to transportation fuels. Understanding the kinetics of kerogen decomposition to oil is critical to designing a viable process. A dataset of thermogravimetric analysis (TGA) of the Green River oil shale is provided and two distinct data analysis approaches—advanced isoconversional method and parameter fitting are used to analyze the data. Activation energy distributions with conversion calculated using the isoconversional method (along with uncertainties) ranged between 93 and 245 kJ/mol. Root mean square errors between the model and experimental data were the lowest for the isoconversional method, but the distributed reactivity models also produced reasonable results. When using parameter fitting approaches, a number of models produce similar results making model choice difficult. Advanced isoconversional method is better in this regard, but maybe applicable to a limited number of reaction pathways. *AIChE J*, 58: 505–515, 2012
Keywords: oil shale/tar sands, petroleum, reaction kinetics

Introduction

Oil shale offers promise as a significant domestic oil source. The Green River formation contains proven vast amounts of oil shale spread among the states of Colorado, Utah, and Wyoming.[1-3] Mahogany zone is one of the richest oil zone intervals.[4] The organic portion of the shale, known as kerogen, undergoes chemical decomposition on thermal heating or retorting to produce a liquid (shale oil). Retorting of oil shale can be performed in different environments. Pyrolysis is a process of heating oil shale in an inert environment. Primary products of pyrolysis are liquid, gas, and coke. The extent of decomposition (yield) and the quality of pyrolysis products depend on the composition of the source material,[5–7] the temperature-time history,[8,9] pressure,[10–12] residence time (secondary reaction),[13,14] and presence of other reactants such as water,[15–18] methane,[19] O_2,[20] CO_2,[21] etc. Because of the chemical composition of the oil produced, moderate to significant upgrading (nitrogen removal and/or hydrogen addition) may be required to convert the oil into a refinery feedstock.[22–24] Producing shale oil of desirable characteristics (low heteroatom content and molecular weight, and high hydrogen) requires an understanding of the decomposition mechanisms and kinetic parameters—activation energy (E), pre-exponential factor (A), and the reaction model [$f(\alpha)$].

TGA analysis of oil shale pyrolysis has appeared in the literature: Colorado oil shale (Green River Formation),[25–27] Spanish oil shale (Puetrollano),[7] Chinese oil shales,[28–30] Pakistani oil shale,[31] Jordanian oil shale,[21] Moroccan oil shale,[32] etc. Elemental analysis and pyrolysis kinetics of oil shales from all over the world were summarized by Nuttall et al.[5] who observed that there were considerable variations in the kinetic parameters of the different shales. A number of researchers have derived relatively simple but effective kinetic expressions for oil evolution during the pyrolysis of Green River and other oil shales based on first-order reaction,[33,34] consecutive first-order reactions,[35] parallel first-order

Correspondence concerning this article should be addressed to M. Deo at milind.deo@utah.edu.

reactions,[36] and logistic or autocatalytic mechanisms.[37] Campbell et al.[34] postulated a first-order decomposition mechanism for the pyrolysis of Colorado oil shale and reported an activation energy of 214.4 kJ/mol and a frequency factor of 2.8 E 13 s^{-1}. Leavitt et al.[36] proposed two parallel first-order lumped reactions and, obtained activation energies of 191.02 kJ/mol for temperature above 350°C and 87 kJ/mol for temperature below 350°C. A controversial two-step mechanism has also been proposed by Braun and Rothman.[38] Burnham[15,39] have argued convincingly by using multiple sets of data that this two step decomposition mechanism is not appropriate for oil shale pyrolysis. More complex kinetic analysis procedures have also been used in deriving kinetics of decomposition of oil shales.[6,40–42] It has also been reported that kinetics parameters obtained using one apparatus do not agree well with those derived using a different system. Burnham[39] notes that these differences are primarily due to the use of poor kinetic analysis methods.

The kinetic analysis round table[43–47] convened to study the kinetics of reactions involving complex solid materials concluded that it was inappropriate to use a single heating rate and a prescribed kinetic model to derive kinetic parameters. The basic flaw in methods which followed this procedure was that they resulted in activation energies that were heating rate dependent. By using a variety of computational methods, the panel observed that isoconversion and multiheating methods were particularly useful in describing kinetics of complex material reactions.[43] Burnham and Braun[48] reviewed various kinetic analysis approaches for obtaining kinetic parameters for reactions involving complex materials. They argue for the use of well-chosen models that are able to fit the data and extrapolate beyond the time-temperature range of the data. For complex materials such as kerogen, generalized distributed reactivity models were found to be suitable. When studying the oil shale pyrolysis data, Burnham and Braun[48] use modified Friedman and the modified Coats and Redfern methods while also using the discrete activation energy model. Burnhan and Dihn[49] also compared the isoconversional methods with models obtained using nonlinear parameter estimation. They concluded that reactivity distribution of parallel reactions involving complex materials can be modeled effectively using either the isoconversional methods or parameter fitting approaches; however, they observed that the isoconversional methods are fundamentally inappropriate for use in modeling competing reactions.

Most of these studies recommended the use of distributed reactivity or similar methods, where the reaction rate is inherently independent of heating rates. Variations in the application of these concepts exist in the literature,[49–52] particularly in the manner in which the equations are solved. One of the first applications of the isoconversion method based on the differential form of the rate equation[53] is the Friedman method. Modifications and applications to different complex materials have been reported.[48,50,54] A general application of this concept is the postulation of a model-free isoconversional method,[55] where a functional form of the reaction model is not presupposed. Extensions of this basic theory in the form of advanced isoconversional method have been applied to a number of complex solid materials.[54,56,57] A comprehensive suite of kinetic analysis models based on the concepts discussed by Burnham and Braun[48] is available for use (Kinetic05).

Table 1. Elemental Analysis of the Green River Oil Shale

Oil Shale Sample	Mean (%)	Standard Deviation
Carbon	17.45	0.26
Hydrogen	1.6	0.08
Nitrogen	0.53	0.06
Sulfur	0.18	0.04
Oxygen	15.69	0.79
H/C % (molar)	1.1	
O/C % (molar)	0.67	

Ten samples were analyzed and the mean and standard deviation are shown.

The purpose of this article is to provide a complete TGA dataset for the pyrolysis of Green River oil shale and to compare the performance of the different kinetic models in being able to match the data. Advanced isoconversional models have not seen widespread use perhaps due to their relative computational complexity. The methodologies for implementation of these models allow computations of parameter uncertainties as well. The sophisticated parameter fitting methods are intuitive and easily implemented. However, selection of a unique model from a number of available choices is sometimes difficult. In this article, the root mean square errors between the experimental and modeling data are compared. Selection of a model has real consequences on process predictions—hence, it is important to understand the advantages and disadvantages of using different models.

Experimental Section

The oil shale samples obtained from the Utah Geological Survey were crushed and screened to 100 mesh (1.49 × 10^{-4} m) size particles. The samples were from the Mahogany zone of the Green River formation. The CHNSO (carbon, hydrogen, nitrogen, sulfur, and oxygen) elemental analyses of the samples were performed using LECO CHNS-932 and VTF-900 units and results are summarized in Table 1. The table lists the values along with the standard deviations. The elemental analysis shows that oil shale obtained is Type I on Van Krevelen classification diagram based on the H/C ratio (1.1) and O/C ratio (0.67).[58] The crushed samples were dried for 4 h at 100°C to remove moisture. There was no significant weight loss during drying, and hence, the samples were used as received after screening to 100 mesh. To study the reaction kinetics, a TGA instrument (TA Instruments Q-500) was used for the entire temperature range of kerogen decomposition in N_2 (pyrolysis) environment. Nonisothermal TGA offers certain advantages over the classical isothermal method because it eliminates the errors introduced by the thermal induction period. Nonisothermal analysis also permits a rapid and complete scan of the entire temperature range of interest in a single experiment.

Results and Discussion

Experimental data

Nonisothermal TGA experiments were performed at heating rates between 0.5 and 50°C/min for the decomposition

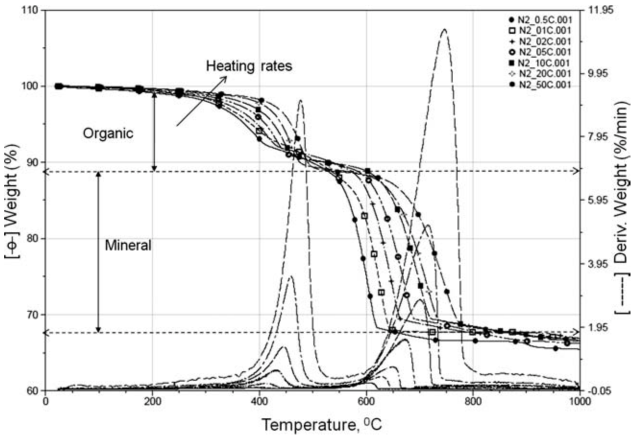

Figure 1. Nonisothermal TGA pyrolysis thermograms: rates go from 0.5°C/min to 50°C/min.

The solid lines are weight loss curves and the dashed lines are derivatives. The arrow indicates that the rates increase as we go from bottom to the top. In the derivative curves, the highest peaks for the highest rate used. The second set of derivative peaks is due to mineral decomposition.

of the crushed and undried oil shale samples (20–30 mg). Weight loss data along with derivatives are shown in Figure 1 for seven (7) heating rates. The mass and temperature measurements in the instrument were calibrated periodically and confirmed with a standard material, calcium oxalate. Excellent reproducibility was observed in the mass loss curves. The TGA kinetics could be affected by different process parameters, such as flow rate, particle size, etc. Galan and Smith[26] concluded that if the particle size was greater than about 4×10^{-4} m and if more than two to three layers of particles were present, transport of heat and mass influence the rate. Hence, the sizes of the particles used along with other conditions used were specifically designed to eliminate heat and mass transfer effects during pyrolysis. The total flow rate of nitrogen gas was 100 ml/min (60 ml/min as purge and 40 ml/min as balance gas).

The total extractable kerogen content in Mahogany oil shale was found to be about 10–12% of the total weight. There was no significant weight loss observed during preheating, confirming the absence of moisture content in the sample. This result was confirmed in TGA experiments, where there was neither significant peak detection nor weight loss below 150°C. Two significant derivative peaks in all nonisothermal experiments were observed, corresponding to organic and carbonate decompositions. The carbonate decomposition commenced at 525°C or above, depending upon the heating rate, and resulted in a total weight loss of about 25–30%. It was also observed that the maximum rate shifts to higher temperatures and decomposition rate increases as the heating rate increases from 0.5 to 50°C/min. This difference is due to shorter exposure time to a particular temperature at faster heating rates (Figure 1). The organic decomposition occurs between 250 and 550°C and depends on heating rate. The data show one single peak for organic decomposition, indicating that one distinguishable process occurs in this temperature range. Nonisothermal experimental conditions and onset analysis criteria such as start, maximum rate and end points are summarized in Table 2.

Kinetic analysis—advanced isoconversional methods

It has been noted in the earlier literature that kerogen is a cross linked, high molecular weight solid.[59,60] During pyrolysis, bonds are broken, leading to multiple reactions. As described earlier, one peak was observed in the organic decomposition temperature range. Consequently, globally single stage decomposition was assumed in deriving kinetic rate expressions.

$$\text{Kerogen} \longrightarrow \text{Decomposition products}$$

Advanced isoconversion methods or sophisticated parameter estimation methods would be appropriate for the analysis of kinetics of decomposition of complex materials like kerogen.[43,49] The salient features of these methods are discussed here.

The conversion of solid matter in shale (kerogen) to products from TGA weight loss data is defined as,[61]

$$\alpha = \frac{W_0 - W_t}{W_0 - W_\infty} \tag{1}$$

In general, the rate of decomposition can be expressed using the non parametric kinetic equation

$$\frac{d\alpha}{dt} = f(T) \cdot f(\alpha) \tag{2}$$

Using Arrhenius expression leads to the following,

Table 2. Analysis Criteria for the Nonisothermal TGA Pyrolysis Data

		Analysis Criteria					
		Start		End		Maximum	
Heating Rate (β)	Initial Weight (mg)	T (°C)	wt % Loss	T (°C)	wt % Loss	T_{max} (°C)	wt % Loss
0.5	22.64	255.6	1.32	421.6	8.02	392.7	6.48
1	28.64	269.6	1.16	437.6	7.48	398.3	5.79
2	26.90	280.0	1.33	456.4	8.43	414.1	6.52
5	25.97	348.9	2.17	474	9.41	432.2	7.17
10	38.45	349.7	1.74	490	9.67	445.6	7.26
20	29.49	371.6	1.58	504	10.68	460.1	7.92
50	22.37	377.3	1.43	530.6	11.13	477.0	7.89

$$\frac{d\alpha}{dt} = f(T) \cdot f(\alpha) = A \cdot e^{\frac{-E}{RT(t)}} \cdot f(\alpha) \tag{3a}$$

Isoconversional methods are specifically designed to address deficiencies in variable heating rate analyses.[43] Advanced model-free isoconversion method has been used in this article. The concepts of advanced isoconversional method and estimation of uncertainty were adapted from a series of papers published by Vyazovkin and Wight, and co-researchers.[54–57,62–64]

For a constant heating rate $\beta = dT/dt$, Eq. 3a can be written as:

$$\beta \cdot \frac{d\alpha}{dT} = A \cdot e^{\frac{-E}{RT(t)}} \cdot f(\alpha) \tag{3b}$$

The direct solution of this equation requires numerical differentiation of the experimental measurements.[54] The integral form of this equation after separating variables is:

$$\int_0^{\alpha^*} \frac{d\alpha}{A \cdot f(\alpha)} = \frac{1}{\beta} \int_0^{T^*} e^{\frac{-E}{RT(t)}} dT = \frac{1}{\beta} [I(E_\alpha, T_\alpha)] \tag{4}$$

There is no known analytical solution to the integral in Eq. 4. Several approximations have been proposed.[65,66] It would also be possible to perform numerical integration using well-established procedures. The assumptions that reaction model does not depend on heating rates and is constant for a small conversion interval lead to the integral form of the rate law (5).

$$\frac{\alpha_{\text{end}} - \alpha_{\text{start}}}{Af(\alpha)} = \frac{I(E_\alpha, T_\alpha)}{\beta} \tag{5}$$

These assumptions suggest that the integral at any particular conversion should be the same for all heating programs and be a function of time-temperature relationship. According to this, for a set of N experiments carried out at different heating programs, the activation energy is determined at any particular level of conversion by minimizing the following function.[54]

$$\chi^2(E) = \frac{1}{N(N-1)} \sum_{i=1}^{N} \sum_{j \neq i} \left(1 - \frac{I_i(E,T)}{I_j(E,T)}\right)^2 \tag{6}$$

Where the subscripts i and j represent two experiments performed under different heating programs. The trapezoidal rule is used to evaluate the integral numerically and the minimization procedure is repeated for each value of α to find the dependence of activation energy on the extent of conversion. The activation energy distribution obtained in Eq. 6 can be used to determine $[A{\cdot}f(\alpha)]$ as a function of α. The confidence intervals for the activation energies and for the values of $A{\cdot}f(\alpha)$ can be calculated using the statistical approach described.[54,64]

The experimental rate and conversion data can be reconstructed based on the model parameters using Eq. 7 below.

$$\ln\left[\beta_i \left(\frac{d\alpha}{dT}\right)_{\alpha,i}\right] = \ln[A \cdot f(\alpha)] - \left(\frac{E_\alpha}{R \cdot T_{\alpha,i}}\right) \tag{7}$$

A MATLAB program using the function ODE45 was used to solve the above ordinary differential equation. $E(\alpha)$ and $[A{\cdot}f(\alpha)]$ which were inputs to the MATLAB program were obtained using the isoconversional analysis described above.

The kinetic models can be used to extrapolate to nonexperimental rates. Slow pyrolysis that is likely during *in situ* oil shale production and high rates of flash pyrolysis are of interest. The assumptions of the isoconversion method (Eq. 5) allow calculating the temperature to reach a level of conversion at extrapolated heating rates using the following mathematical equivalency,[56]

$$\frac{I(E_\alpha, T_{\alpha,i})}{\beta_i} = \frac{I(E_\alpha, T_{\alpha,j})}{\beta_j} \tag{8}$$

The equation above was used to estimate the temperature at which the material starts to convert. The procedure for reconstruction was then used to obtain conversions and rates at extrapolated conditions. One of the advantages of using the advanced isocoversional approach is that uncertainties in E values can also be estimated.

Kinetic analysis—advanced parameter fitting approaches

Results from other parameter fitting models were compared with those obtained with advanced isoconversional method. The Kinetic05 package developed by Braun and Burnham at Lawrence Livermore National Laboratory and supplied by GeoIsoChem is capable of obtaining kinetic parameters of a variety of models. These include the power law and the distributed reactivity models. TGA or other thermal analysis data can be used. Distributed reactivity model options include the Friedman-based isoconversional method, Gaussian and Weibull distributions, and a few others. The application of these models were discussed by Burnham and Braun[48] for different complex materials. In Kinetic05, the model parameters are refined by minimizing the residual sum of squares between observed and calculated reaction data by using nonlinear regression. The details of mathematical formulas and solution procedures have been published previously.[48]

Kinetic analysis results—advanced isocoversional method

The TGA data were normalized from 0 to 1 before analysis. The temperature at which the derivative of weight loss starts to rise was chosen as the zero conversion point, and the temperature at which the weight derivative returned to the base line was the end point. Isokin, a package developed at the University of Utah,[54] was used for the calculation of the distribution of activation energies and other kinetic parameters. Distributions in kinetic parameters, E and $A{\cdot}f(\alpha)$ were determined as functions of conversion.

The confidence interval estimation was performed by using different number of heating rates and/or different combinations of heating rates. Uncertainties were calculated for

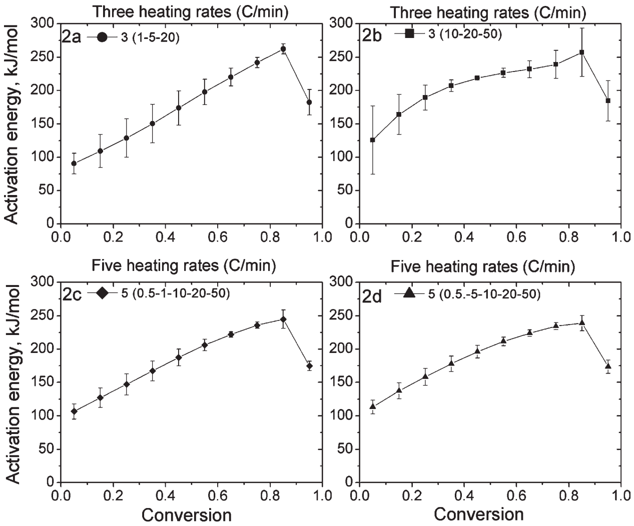

Figure 2. Distribution of activation energies for pyrolysis of Green River oil shale calculated using the advanced isoconversional method.

The uncertainties in activation energy values are shown for different numbers of heating rates considered and for different combinations. As all of the heating rates are used, uncertainties are reduced over the entire conversion range (d). The final calculation of activation energies with uncertainties are shown in Figure 3a.

10 conversion intervals for different cases (Figures 2a–d). Uncertainty values increased when fewer rates were used. When heating rates spanning the wider range (e.g., 50°C/min and 0.5°C/min) were included in sparse data sets, the uncertainties were generally lower. Figure 3a shows activation energy distribution (as a function of conversion) and associated uncertainties when all the seven heating rates were employed. Figure 3b shows $A{\cdot}f(\alpha)$ as a function of conversion. Activation energies ranged from 93 to 245 kJ/mol. The values of $A{\cdot}f(\alpha)$ varied from 1.42 E 6 to 4.46 E 16 min^{-1}. The kinetic parameters estimated in this work are consistent with those observed by others for Green River oil shale.[33,34] For Kukersite shales, which was considered a ‘‘standard’’ because of reproducibility, the activation energies ranged from 210 to 234 kJ/mol.[48] The values of activation energies reported in this work of about 93–245 kJ/mol are lower at lower conversions.

It is argued[67] that the variation in activation energy for the decomposition of a complex material is caused by the fact that the overall rate measured by thermal analysis is a combination of the rates of several parallel reactions, each of which has its own energy barrier, and hence an activation energy. The effective activation energy derived from these global rate measurements becomes a function of the individual activation energies.

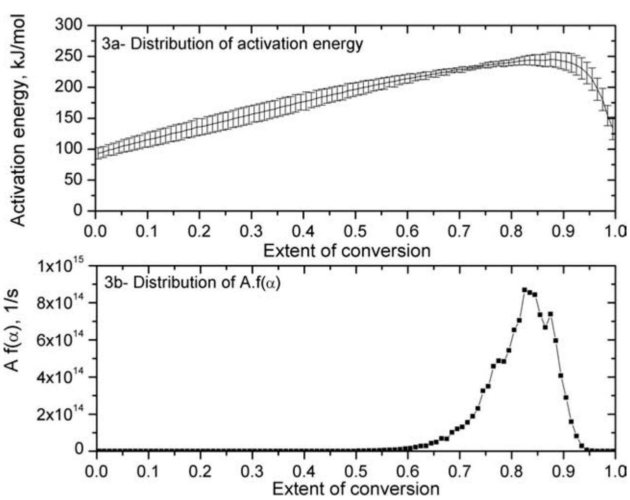

Figure 3. Distribution of kinetic parameters with extent of conversion [(a) activation energy (b) $A{\cdot}f(\alpha)$] determined using the advanced isoconversional method.

All of the seven rates were used in calculating the kinetic parameters. Uncertainties in activation energy values are also shown.

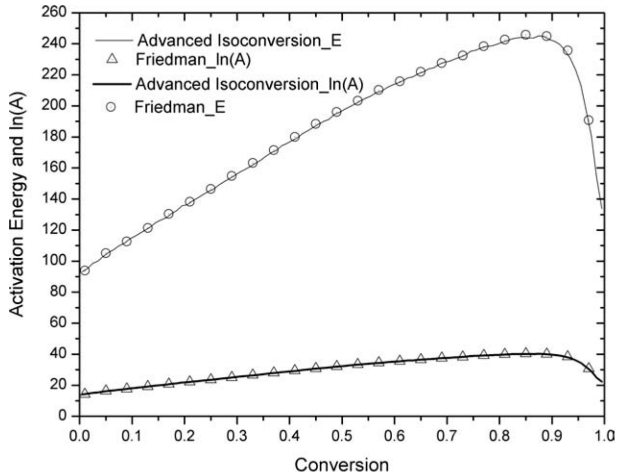

Figure 4. Comparison of kinetic parameters from advanced isoconversional and the Friedman method.

The kinetic model is assumed to be first order for this comparison.

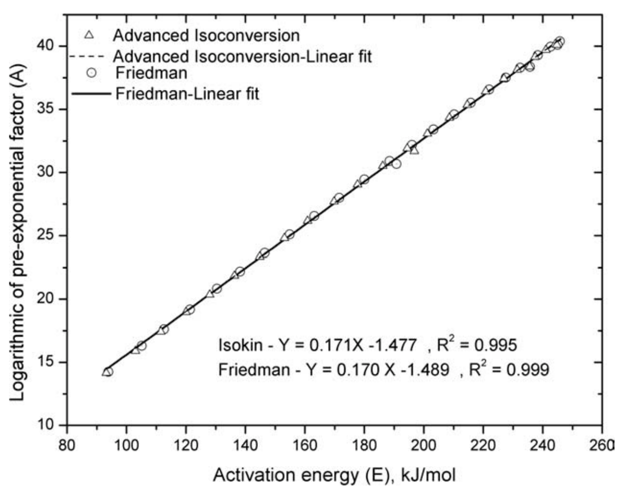

Figure 5. Constable plots for Friedman and advanced isoconversional kinetic parameters.

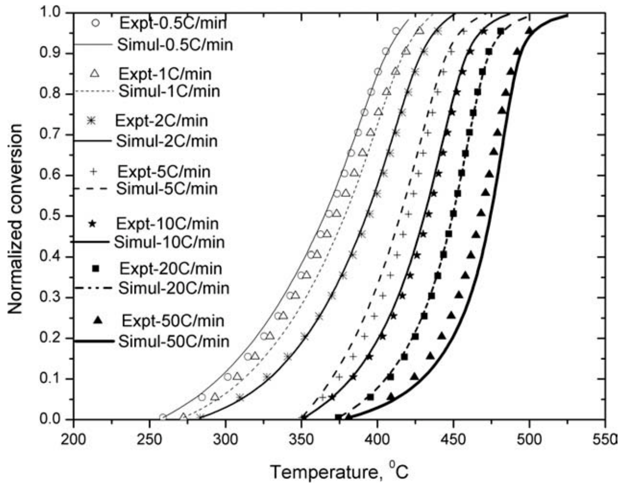

Figure 6. Experimental and simulated conversion profiles at different heating rates using the advanced isoconversional method.

MATLAB-based computational method described in the text was used.

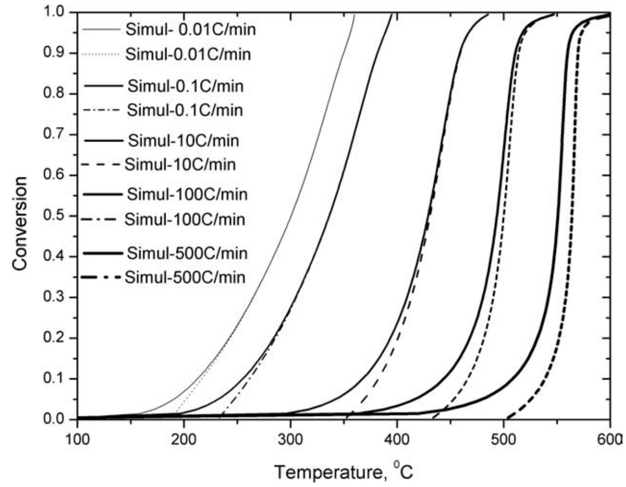

Figure 7. Simulated conversion profiles at extrapolated constant heating rates using two different initial temperatures.

Continuous lines show profiles with $T_0 = 100°C$ and dotted lines depict extrapolations with T_0 calculated from Eq. 8.

Advanced isoconversion method provides combined pre-exponential factor and reaction model as function of conversion. The values of pre-exponential factor A can be calculated after assuming a reaction model (order, functionality, etc.). For example, the Friedman method assumes a first-order reaction, and using the functionality of $(1 - \alpha)$ for $f(\alpha)$, A can be calculated. A graphical implementation of the Friedman approach also yields $E(\alpha)$ and A as functions of conversion. The comparison of kinetic parameters obtained from Isokin first-order model and Friedman graphical method are depicted in Figure 4. The agreement between kinetic parameters obtained using the two approaches is excellent. The results support that thermal decomposition pyrolysis of Mahogany oil shale is globally a first-order process. This is also confirmed by observing the Constable plot, that examines the relationship between logarithm of A and E.[68] The linear (or near-linear) profile in the Constable plot may be adequate[62] to confirm the order of the reaction. The Constable plots shown in Figure 5 are remarkably linear confirming the order to be unity for both the approaches used.

The distributions of E and $A{\cdot}f(\alpha)$ were used in model equations to recreate the experimental data. A MATLAB code with the ODE45 solver was used in the calculations. In the practical implementation of the code, temperature was the dependent variable. Results of the model comparisons with the experimental data are shown in Figure 6. The agreement between the model and the experimental data is good over most of the conversion range, and for all the rates. The experimental data at 10°C/min were used as basis to calculate the conversion profiles for rates at which experimental data was not available. Extrapolated profiles at rates ranging from 0.01°C/min to 500°C/min are shown in Figure 7. At slow heating rates, decomposition begins at lower temperatures, whereas in the fast pyrolysis, the products are released at higher temperatures. Simulated decomposition rates and onset temperatures shift to higher temperatures at higher-heating rates. The extrapolated results are not all consistent with some experimental results. To explain all aspects of the extrapolated profiles, introduction of reaction initiation type mechanisms[14,69] proposed by a few researchers may have to be considered.

Kinetic analysis results—advanced parameter fitting models

The models from Kinetic05 used for comparison purposes are listed in Table 3. Table 3 also shows the parameters obtained. The power law model was applied in two cases: first-order and *n*th-order. In the latter case, optimal values of n, E, and A were obtained using nonlinear regression. The *n*th-order reaction model is mathematically equivalent to

Table 3. Parameters Obtained Using Selected Kinetic Models Available in Kinetic05

Kinetic Models		E (kJ/mol)	A (1/s)	Order	Parameter 1	Parameter 2
Gaussian	$n = n$	180.061	8.12E E 10	0.53	4.19 E +00	
	$n = 1$	181.446	1.29 E +11	1.00	3.78 E +00	
Discrete	Case 1	Figure 8(a)	5.72 E +09	1.00		
	Case 2	Figure 8(b)	1.00 E +14	1.00		
	Case 3	Figure 8(c)	$e^{(a + bE)}$	1.00		
Weibull		163.154	6.64 E +09	1.00	1.04 E +04	9.99 E +00
First order		156.968	2.19 E +09	1.00		
*n*th order		160.735	5.80 E +09	1.65	1.65	
Isoconversional		Figure 4		1	Friedman based	

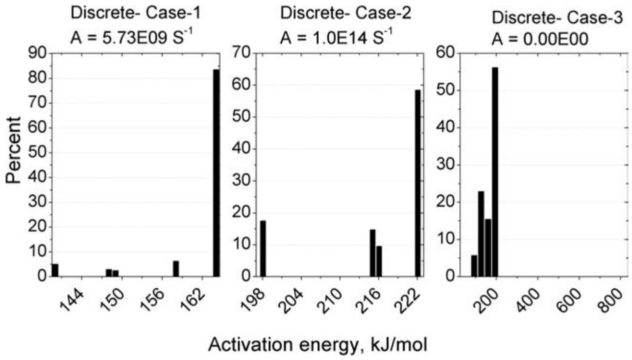

Figure 8. Distribution of activation energies from discrete reactivity models (Cases 1–3 as described in the text).

Gamma distribution.[70] The Gaussian distribution approach used by Braun and Burnham[71] was also used with the first and the *n*th-order models. Discrete reactivity distribution models are based on different combinations of A and E assuming the reaction to be first order. Three different cases were used in this work, and the results were compared:

1. Fixed E-spacing;
2. Initial A-range and fixed E-spacing; and
3. Constable relationship for A and E, ($\ln(A) = a + bE$).

The distributions of activation energies from discrete models are shown in Figure 8. The three different approaches produced different kinetic parameters. Use of Weibull distribution is another parameter fitting method used extensively for petroleum source rocks by Lakshmanan and White.[72] Isoconversional method in Kinetic05 is based on the first-order Friedman-type of analysis. The distribution of activation energies obtained using this approach in Kinetic05 is almost identical to the distribution obtained using the advanced isoconversional method (Figure 4). The reconstruction of conversion and rate experimental data using different Kinetic05 models and Isokin were compared at all experimental heating rates. The results are shown for a heating rate of 10°C/min in Figure 9. The general trend is that the cumulative conversions are matched reasonably well while the rates have higher discrepancies.

Comparison of the different kinetic models used

The comparison of the sum of the root mean square (RMS) errors (all seven experimental heating rates) is shown in Figure 10 (Figure 10a for reaction rates and Figure 10b for conversions). The errors were calculated for 100 points of conversion at the same values of experimental temperatures. The RMS values are lower for the advanced isoconversional method compared with the parameter fitting and reactivity distribution models. The isoconversional approach from Kinetics05 also produced RMS values comparable with the ones shown for the advanced isoconversional method. The parameter fitting approaches, particularly with discrete activation energies also result in reasonable RMS values. The parameter fitting approaches may result in determination of parameter sets that are nonunique. For example, the first-order and *n*th-order models with Gaussian distribution are characterized by different parameter sets (Table 3), but produce about the same goodness of fit (Figure 10). When this happens, model discrimination becomes an issue. However, these models are flexible and can be used with any reaction combinations (parallel, series, etc.). The isoconversion

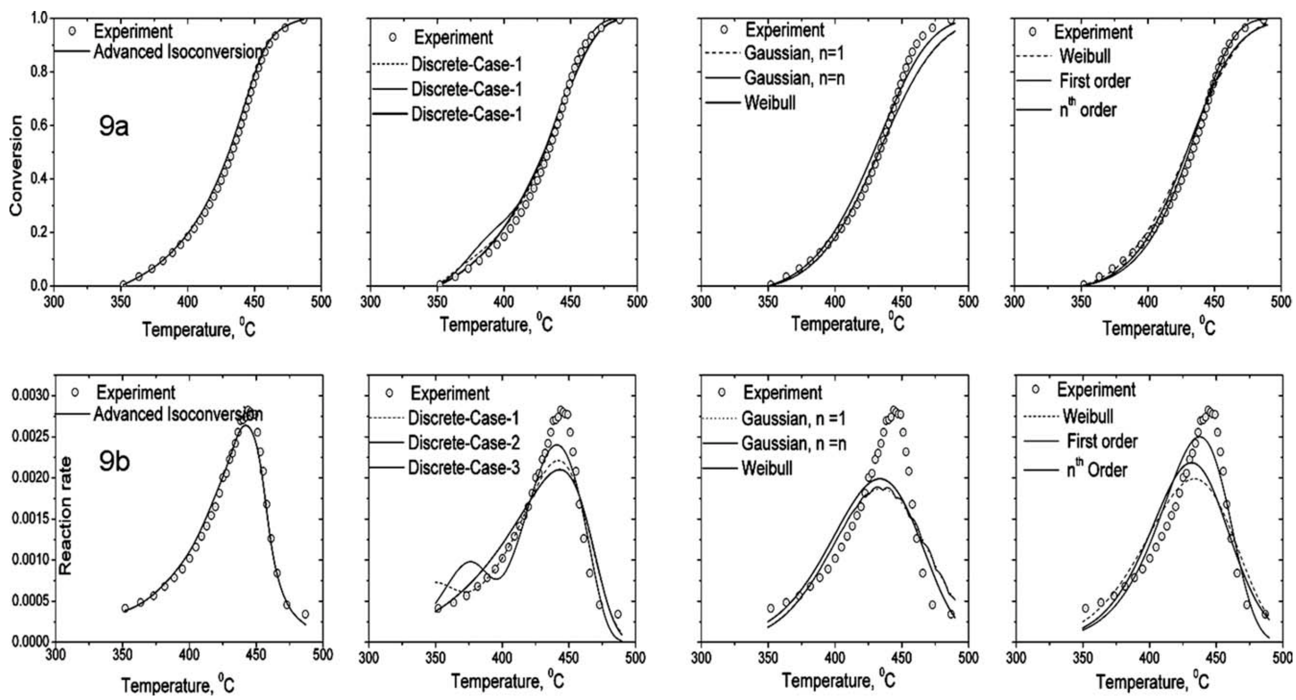

Figure 9. Comparison of different kinetic models at a heating rate of 10°C/min [panel (a) conversion and panel (b) reaction rate].

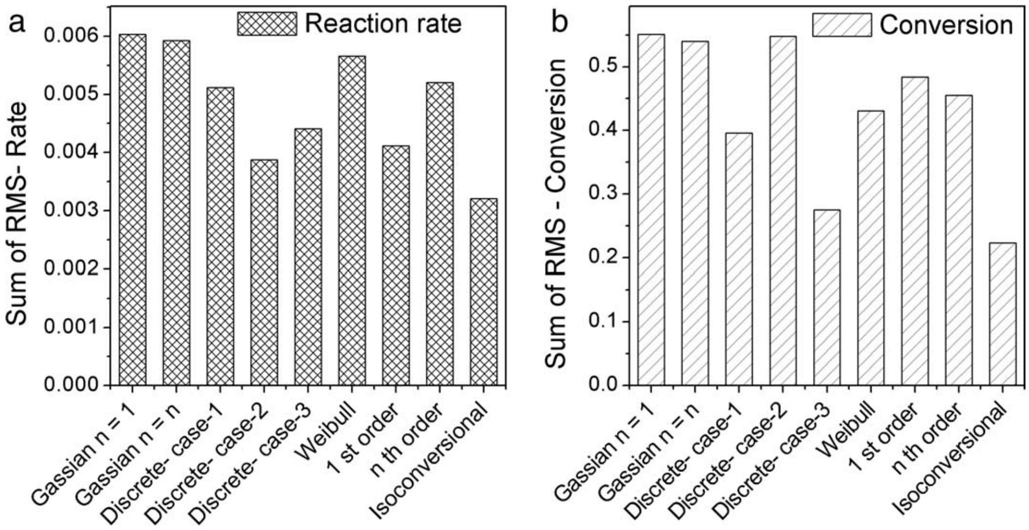

Figure 10. Comparison of different kinetic models based on sum of root mean square (RMS) residues.

In all these calculations, 100 experimental data points were used. RMS is summed over all of the seven experimental heating rates.

approach which does not consider a kinetic model *a priori* gets around this, but may not be as flexible as the parameter fitting methods. Burnham and Dinh[49] argue that isocovension models are not suitable for modeling reactions in series.

The kinetic parameters obtained from different models were used to extrapolate the data outside of the experimental range. The resulting profiles are compared in Figure 11 for conversion and reaction rate at a heating rate of 100°C/min. Conversion profiles are also shown in Figure 12 for a heating rate of 0.01°C/min. The high heating rates would be applicable for a flash pyrolysis process, whereas the slow heating rates are likely in *in situ* heating of oil shale deposits. These figures show that there are discernible consequences when the models are used to extrapolate the data. At high heating rates, decomposition begins at much higher temperatures when the isoconversional model is used. This trend is consistent with what is observed in the TGA. The peak rates and the temperature range over which the reactions occur (spread of the rate curve) are better reproduced when the isoconversion method is used. Similarly, at lower-heating rates, conversion begins at a lower temperature when the isoconversional model is used. The better performance of the isoconversion model is attributed to the fact that it follows the progress of reactions on the relevant conversion intervals.

Conclusions

In this article, we present a thermogravimetric analysis data of oil shale pyrolysis at seven different heating rates. Derivatives of the weight loss curves show a single major peak in the organic weight loss region indicating that the decomposition is governed by single global mechanism. Kinetic methods found suitable for the analysis of reactions of

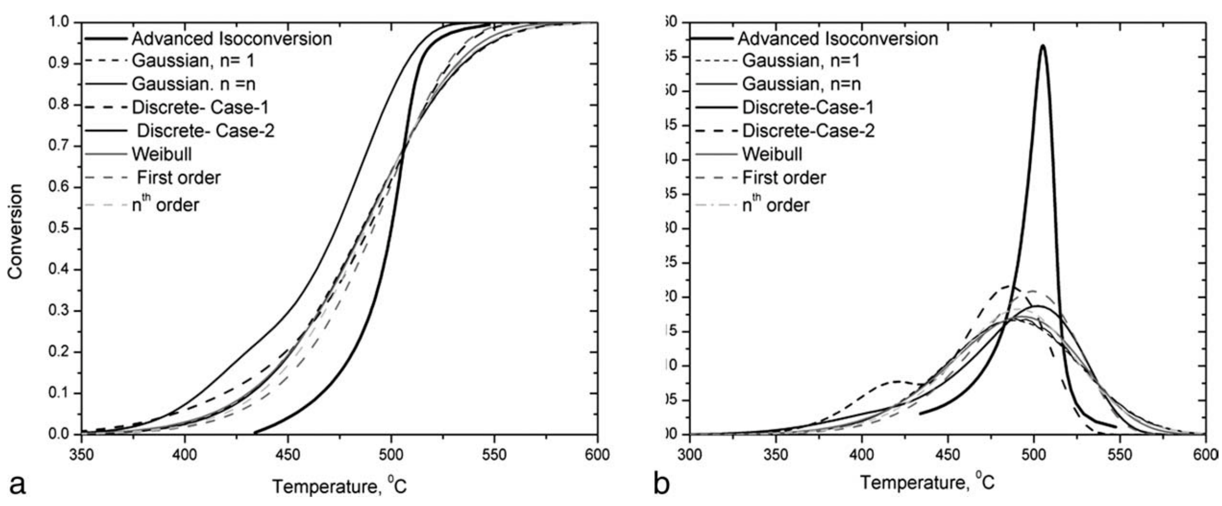

Figure 11. Comparison of different kinetic models at a heating rate of 100°C/min [(a) conversion and (b) reaction rate].

It is seen that under fast pyrolysis conditions, model of choice does have significant impact on predictions.

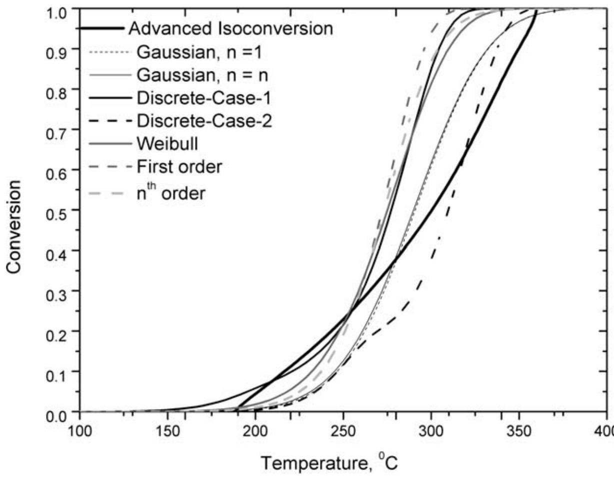

Figure 12. Comparison of the conversion profiles from different kinetic models at a heating rate of 0.01°C/min.

The rates for *in situ* operations are usually slower than this. At these slow rates, also choice of the model used is important in understanding the rate of conversion of oil shale.

complex materials were used to analyze the data and derive kinetic parameters. The advanced isoconversional method yielded activation energies as function of conversion in the range of 93–245 kJ/mol. The decomposition process can be viewed as consisting of multiple parallel reactions with individual activation energies. Maximum uncertainties in activation energies computed using the advanced isoconversion method were about 10% of the energy values calculated. Kinetic parameters were also derived for a few other selected models using parameter fitting programs. The RMS errors between the experimental and model values for the different approaches were compared. The isoconversion approach produced the lowest RMS values in both rates and cumulative conversion (for all of the heating rates, combined), but the parameter fitting approaches also produced reasonable duplication of the data. The parameter fitting approaches using power law, activation energy distribution, or discrete energy values in specific conversion intervals are intuitive and fast. However, model selection is difficult because numerous models produce equivalent results. Change in one parameter (e.g., order) is compensated by changes in activation energies or pre-exponential factors to produce comparable RMS values. Isoconversion models are in theory ''kinetic model'' free and their applicability to the decomposition of a complex material like kerogen is excellent. However, their applicability in reproducing multistep kinetics has been questioned. Application of these models to real life processes requires extending these models outside of the experimental data range from which they were derived. It is shown that the choice of the right model is of great consequence since model predictions outside of the experimental range vary considerably between the models chosen. Even though this analysis has been conducted with oil shale, the approach and conclusions are likely to be applicable to other complex materials.

Acknowledgments

The authors would like to acknowledge financial support from the U.S. Department of Energy, National Energy Technology Laboratory—Grant number: DE-FE0001243. The samples were provided by Utah Geological Survey. The authors thank Professor Wight for providing the Isokin Software developed at the University of Utah for use. They also thank Dr. Burnham of American Shale Oil Company for providing key papers and insight to the kinetic models through various discussions.

Notation

A = frequency (pre-exponential) factor (min^{-1})
E = activation energy (kJ mol^{-1})
E_α = activation energy at conversion α
$f(\alpha)$ = reaction model
$f(T)$ = temperature dependency of the reaction rate
I = integral symbol
N = number of heating rates
R = gas constant (8.314 kJ mol^{-1} K^{-1})
T = temperature (K)
T_0 = initial temperature
T_m = temperature when reaction rate is maximum
T_α = temperature at conversion α
W_0 = initial weight of the sample (mg)
W_t = weight of the sample at time, t (mg)
W_∞ = weight of the sample at the end of the experiment (mg)
α = conversion
β = constant heating rate (°C/min)

Literature Cited

1. Smith JW. *Oil Shale Resources of the United States*, Vol. 23. *CSM Mineral and Energy Resources Series*, Colorado school of Mines, CO, 1980.
2. Dyni JR. Geology and resources of some world oil shale deposits. *Oil Shale*. 2003;20:193–252.
3. Bartis JT, LaTourrette T, Dixon L, Peterson DJ, Cecchine G. *Oil Shale Development in the United States: Prospective and Policy Issues*. RAND Corporation: Santa Monica, CA, 2005.
4. VandenBerg MD. *Basin-Wide Evaluation of the Uppermost Green River Formation's Oil-Shale Resource*. Unita Basin, Utah and Colorado: Utah Geological Survey, 2008.
5. Nuttall HE, Guo T, Schrader S, Thakur DS.*Pyrolysis kinetics of several key world oil shales*. In: Miknis FP, McKay JF, editors. *Geochemistry and Chemistry of Oil Shales*, Vol. 230. Washington DC: American Chemical Society, 1983:269–300.
6. Burham AK, Richardson JH, Coburn TT. Pyrolysis kinetics for western and eastern oil shale. In: *Proceedings of the 17th Intersociety Energy Conversion Engineering Conference*, New York, 1982.
7. Torrente MC, Galan MA. Kinetics of the thermal decomposition of oil shale from puertollano (Spain). *Fuel*. 2001;80:327–334.
8. Burnham AK. Oil evolution from a self-purging reactor: kinetic and composition at 2°C/min and 2°C/h. *Energy Fuels*. 1991;5:205–214.
9. Charlesworth JM. Oil shale pyrolysis. I. Time and temperature dependence of product composition. *Ind Eng Chem Process Des Dev*. 1985;24:1117–1125.
10. Burnham AK, Singleton MF.*High-pressure pyrolysis of green river oil shale*. In: Miknis FP, McKay JF, editors. *Geochemistry and Chemistry of Oil Shales*. Washington DC: American Chemical Society 1983:335–351.
11. Sohn HY, Yang HS. Effect of reduced pressure on oil shale retorting. I. Kinetics of oil generation. *Ind Eng Chem Process Des Dev*. 1985;24:265–270.
12. Yang HS, Sohn HY. Mathematical analysis of the effect of retorting pressure on oil yield and rate of oil generation from oil shale. *Ind Eng Chem Process Des Dev*. 1985;24:274–280.
13. Stainforth JG. Practical kinetic modeling of petroleum generation and expulsion. *Mar Petrol Geol*. 2009;26:552–572.
14. Burnham AK, Happe JA. On the mechanism of kerogen pyrolysis. *Fuel*. 1983;63:1353–1356.

15. Burnham AK. Relationship between hydrous and ordinary pyrolysis. In: *NATO Advanced Study Institute on Composition, Geochemistry and Conversion of Oil Shales Conference,* Akcay, Turkey, 1995.
16. Pan C, Geng A, Zhong N, Liu J, Yu L. Kerogen pyrolysis in the presence and absence of water and minerals. I. Gas components. *Energy Fuels.* 2008;22:416–427.
17. Lewan MD, Ruble TE. Comparison of petroleum generation kinetics by isothermal hydrous and non-isothermal open system pyrolysis. *Org Geochem.* 2002;33:1457–1475.
18. Michels R, Landaisa P, Torkelsonb BE, Philpc RP. Effects of effluents and water pressure on oil generation during confined pyrolysis and high-pressure hydrous pyrolysis. *Geochim Cosmochim Acta.* 1995;59:1589–1604.
19. Hill GR, Johnson DJ, Miller L, Dougan JL. Direct production of low pour point high gravity shale oil. *Ind Eng Chem Prod Res Dev.* 1967;6:52–59.
20. Haung ETS. Retorting of single oil shale blocks with nitrogen and air. *Soc Petrol Eng J.* 1977;17:331–336.
21. Jaber JO, Probert SD. Non-isothermal thermogravimetry and decomposition kinetics of two Jordian oil shales under different processing conditions. *Fuel Process Technol.* 2000;63:57–70.
22. Kavianian HR, Yesavage VF, Dickson PF, Peters RW. Kinetic simulation model for steam pyrolysis of oil shale feedstock. *Ind Eng Chem Res.* 1990;29:527–534.
23. Fathoni AZ, Batts BD. A literature review of fuel stability studies with a particular emphasis on shale oil. *Energy Fuels.* 1992;6:681–693.
24. Utah Heavy Oil Program. A technical, economical and legal assessment of North American heavy oil, oil sands, and oil shale resources. In response to Energy Policy Act of 2005 Section 369(p). Utah Heavy Oil Program: University of Utah, Salt Lake City, UT, 2007.
25. Rajeshwar K. The kinetics of the thermal decomposition of green river oil shale kerogen by non-Isothermal thermogravimetry. *Thermochim Acta.* 1981;45:253–263.
26. Galan MA, Smith JM. Pyrolysis of oil shale: experimental study of transport effects. *AIChE J.* 1983;29:604–610.
27. Hillier J, Fletcher J, Orgill J, Isackson C, Fletcher TH. An improved method for determination of kinetic parameters from constant heating rate TGA oil shale pyrolysis data. *Prepr Pap Am Chem Soc Div Fuel Chem.* 2009;54:155–157.
28. Li S, Yue C. Study of pyrolysis kinetics of oil shale. *Fuel.* 2003;82:337–342.
29. Li S, Yue C. Study of different kinetic models for oil shale pyrolysis. *Fuel Process Technol.* 2003;85:51–61.
30. Qing W, Baizhong S, Aijuan H, Jingru B, Shaohua L. Pyrolysis characteristic of Huadian oil shale. *Oil Shale.* 2007;24:147–157.
31. William PT, Ahmad N. Influence of process conditions on the pyrolysis of Pakistani oil shale. *Fuel.* 1999;78:653–662.
32. Thakur DS, Nuttal HE. Kinetics of pyrolysis of Moroccan oil shale by thermogravimetry. *Ind Eng Chem Process Des Dev.* 1987;26:1351–1356.
33. Shin SM, Sohn HY. Nonisothermal determination of the intrinsic kinetics of oil generation from oil shale. *Ind Eng Chem Process Des Dev.* 1980;19:420–426.
34. Campbell JH, Koskinas GH, Stout ND. Kinetics of oil generation from Colorado oil shale. *Fuel.* 1978;57:372–376.
35. Hubbard AB, Robinson WE. *A Thermal Decomposition Study of Colorado Oil Shale, Report of Investigation #4744*. Washington DC: U.S. Bureau of Mines 1954.
36. Leavitt DR, Tyler AL, Kafesjiant AS. Kerogen decomposition kinetics of selected green river and eastern U.S. oil shales from thermal solution experiments. *Energy Fuels.* 1987;1:520–525.
37. Allred VD. Kinetics of oil shale pyrolysis. *Chem Eng Prog.* 1966;62:55–60.
38. Braun RL, Rothman AJ. Oil shale pyrolysis: kinetics and mechanism of oil production. *Fuel.* 1975;54:129–131.
39. Burnham AK. *Chemistry and Kinetics of Oil Shale Retorting*. In: Ogunsola OI, Hartstein AM, Ogunsola O. editors. *Oil Shale: A Solution to the Liquid Fuel Dilemma*, Vol. 1032. Washington DC: ACS Symposium Series, 2010:115–134.
40. Braun RL, Burnham AK. Analysis of chemical reaction kinetics using a distribution of activation energies and simpler models. *Energy Fuels.* 1987;1:153–161.
41. Burnham AK, Braun RL. General kinetic model of oil shale pyrolysis. *In Situ.* 1985;9:1–23.
42. Burnham AK, Braun RL, Coburn TT, Sandvik EI, Curry DJ, Schmidt BJ, Noble RA. An appropriate kinetic model for well-preserved algal kerogen. *Energy Fuels.* 1996;10:49–59.
43. Brown ME, Maciejewski M, Vyazovkin S, Nomen R, Sempere J, Burnham A, Opfermann J, Strey R, Anderson HL, Kemmeler A, Janssens J, Desseyn HO, Li CR, Tang TB, Roduit B, Malek J, Mitsuhasshi T. Computational aspects of kinetic analysis, part A. The ICTAC kinetics project—data, methods and results. *Thermochim Acta.* 2000;355:125–143.
44. Burnham AK. Computaional aspects of kinetic analysis, part D. The ICTAC kinetic project—multi-thermal-history model fitting methods and their relation to isoconversion methods. *Thermochim Acta.* 2000;355:165–170.
45. Maciejewski M. Computational aspects of kinetic analysis, part B. The ICTAC project—the decomposition kinetics of calcium carbonate revisited, or some tips on survival in the kinetic minefield. *Thermochim Acta.* 2000;355:125–143.
46. Roudit B. Computational aspects of kinetic analysis, part E. Numerical techniques and kinetics of solid state processes. *Thermochim Acta.* 2000;35:171–180.
47. Vyazovkin S. Computational aspects of kinetic analysis, part C. The ICTAC project—the light at the end of the tunnel?*Thermochim Acta.* 2000;355:155–163.
48. Burnham AK, Braun RL. Global kinetic analysis of complex materials. *Energy Fuels.* 1999;13:1–22.
49. Burnham AK, Dinh LN. A comparison of isoconversional and model-fitting kinetic parameter estimation and application predictions. *J Therm Anal Calorim.* 2007;89:479–490.
50. Starink MJ. The determination of activation energy from linear heating rate experiments: a comparison of the accuracy of isoconversion methods. *Thermochim Acta.* 2003;404:163–176.
51. Sundararaman P, Merz PH, Mann RG. Determination of kerogen activation energy distribution. *Energy Fuels.* 1992;6:793–803.
52. Al-Ayed OS, Matouq M, Anbar Z, Khaleel AM, Abu-Nameh E. Oil shale pyrolysis kinetics and variable activation energy principle. *Appl Energy.* 2010;87:1269–1272.
53. Friedman HL. Kinetics of thermal degradation of charforming plastics from thermogravimetry. Application to a phenolic plastic. *J Polym Sci Part C: Polym Symp.* 1964;6:183–195.
54. Vyazovkin S, Wight CA. Estimating realistic confidence intervals for the activation energy determined from thermoanalytical measurements. *Anal Chem.* 2000;72:3171–3175.
55. Vyazovkin S, Wight CA. Isothermal and non-isothermal kinetics of thermally stimulated reactions of solids. *Int Rev Phys Chem.* 1998;17:407–433.
56. Vyazovkin SV, Lesnikovich AL. Practical application of isoconversional methods. *Thermochim Acta.* 1992;203:177–185.
57. Vyazovkin S, Wight CA. Kinetics in solids. *Annu Rev Phys Chem.* 1997;48:125–149.
58. Hutton A, Bharati S, Robl T. Chemical and petrographical classification of kerogen/macerals. *Energy Fules.* 1994;8:1478–1488.
59. Behar F, Vandenbroucke M. Chemical modelling of kerogens. *Org Geochem.* 1987;11:15–24.
60. Vandenbroucke M, Largeau C. Kerogen origin, evaluation and structure. *Org Geochem.* 2007;38:719–833.
61. Blazek A.*Thermal analysis*. In: Tyson JF, editor. *Thermal Analysis.* London: Van Nostrand Reinhold, 1973.
62. Vyazovkin SV, Lesnikovich AL. Estimation of the pre-exponential factor in the isoconversional calculation of effective kinetic parameters. *Thermochim Acta.* 1988;128:297–300.
63. Vyazovkin S, Linert W. Detecting isokinetic relationships in non-isothermal systems by the isoconversional method. *Thermochim Acta.* 1995;269/270:61–72.
64. Vyazovkin S, Sbirrazzuoli N. Confidence intervals for the activation energy estimated by few experiments. *Anal Chim Acta.* 1997;355:175–180.
65. Doyle CD. Estimating isothermal life from thermogravimetric data. *J Appl Polym Sci.* 1962;6:639–642.
66. Senum GI, Yang RT. Rational approximations of the integral of the Arrhenius function. *J Therm Anal Calorim.* 1977;11:445–447.
67. Vyazovkin S. Reply to "What is meant by the term 'variable activation energy' when applied in the kinetics analyses of solid state decompositions (crystolysis reactions)?" *Thermochim Acta.* 2003; 397:269–271.

68. Constable FH.*The mechanism of catalytic decomposition*. In: *Proceedings of the Royal Society of London*. Vol. 108. London: The Royal Society, 1923:355–378.
69. Charlesworth JM. Oil shale pyrolysis, part 2. Kinetics and mechanism of hydrocarbon evolution. *Ind Eng Chem Process Des Dev*. 1985;24:1125–1132.
70. Boudreau BP, Ruddick BR. On a reactive continuum representation of organic matter diagenesis. *Am J Sci*. 1991;291:507–538.
71. Burnham AK, Braun RL, Gregg HR. Comparison of methods for measuring kerogen pyrolysis rates and fitting kinetic parameters. *Energy Fuels*. 1987;1:452–458.
72. Lakshmanan CC, White N. A new distributed activation-energy model using weibull distribution for the representation of complex kinetics. *Energy Fuels*. 1994;8:1158–1167.

Manuscript received Sept. 13, 2010, and revision received Jan. 14, 2011.